Electrochemical detection of redox molecules secreted by Pseudomonas aeruginosa – Part 1: Electrochemical signatures of different strains

Julie Oziat, Thibaut Cohu, Sylvie Elsen, Maxime Gougis, George Malliaras, Pascal Mailley

Electrochemical detection of redox molecules secreted by *Pseudomonas aeruginosa* – Part 1: Electrochemical signatures of different strains

Julie Oziat [a,b,c], Thibaut Cohu [a], Sylvie Elsen [d], Maxime Gougis [a], George G. Malliaras [b,e], Pascal Mailley [a,*]

[a] *Univ. Grenoble-Alpes, CEA Leti, MINATEC Campus, F-38054 Grenoble, France*
[b] *Department of Bioelectronics, Ecole Nationale Supérieure des Mines de Saint-Etienne, F-13541 Gardanne, France*
[c] *Bioserenity, Institut du Cerveau et de la Moelle Epinière, 47 Bd de l'Hôpital, 75013 Paris, France*
[d] *UMR 1036, INSERM-CEA-UJF, CNRS ERL5261, BIG, CEA-Grenoble, F-38054 Grenoble, France*
[e] *Electrical Engineering Division, Department of Engineering, University of Cambridge, Cambridge CB3 0FA, UK*

ARTICLE INFO

ABSTRACT

During infections, fast identification of the microorganisms is critical to improve patient treatment and to better manage antibiotics use. Electrochemistry exhibits several advantages for rapid diagnostic: it enables easy, cheap and *in situ* analysis of redox molecules in most liquids. In this work, several culture supernatants of different *Pseudomonas aeruginosa* strains (including PAO1 and its isogenic mutants PAO1Δ*pqsA*, PA14, PAK and CHA) were analyzed by square wave voltammetry on glassy carbon electrode during the bacterial growth. The obtained voltamograms shown complex traces exhibiting numerous redox peaks with potential repartitions and current amplitudes depending on the studied bacterium and/or growth time. Among them, some peaks were clearly associated to the well-known redox toxin Pyocyanin (PYO) and the autoinducer Pseudomonas Quinolone Signal (PQS). Other peaks were observed that are not yet attributed to known secreted species. Each complex electrochemical response (number of peaks, peak potential and amplitude) can be interpreted as a fingerprint or "ID-card" of the studied strain that may be implemented for fast bacteria strain identification.

Published by Elsevier B.V.

1. Introduction

Detection and identification of pathogenic bacteria is of main importance in clinical diagnostics, food processing or water quality management. Reference methods for bacteria identification are either time-consuming, such as classical cultures on Petri dishes. Other are complex and expensive such as PCR-based detection strategies. Early *in situ* real-time identification would enable rapid treatment to avoid proliferation and further possible contamination of humans or animals. Moreover, this would enable better antibiotic management, leading to substantial societal and economical gains [1]. Bacteria are known to secrete a wide range of small (bio)molecules (including proteins, peptides, lipids and small organic compounds) involved in or/and issued from their communication process, metabolism or virulence [2,3]. This secretome is specific to each bacterium and can be used for *in situ* detection and identification in water analysis, food processing or diagnostics (measurements in biological fluids, serum, whole blood, saliva, urine). Contrary to others strategies, like microgravimetry, electro-

chemical impedance spectroscopy or surface plasmon resonance, detecting (bio)molecules secreted by a bacterium has the tremendous advantage to do not need any specific bioreceptor.

Bacterial secretome is widely studied for different pathogenic bacteria including *Pseudomonas aeruginosa* [4,5]. These studies are mainly focused on the identification of the different species present in the secretome and their implication in the bacterial regulation process or virulence. These analyses require generally complex apparatus including HPLC and mass spectrometry [6] that are impossible to miniaturize with the aim of *in situ* real time detection. Within the secretome (bio)molecules, some species present a redox behavior that could be exploited for analytical purpose using electroanalysis. For example, *P. aeruginosa* is known to specifically produce the blue redox-active virulence factor Pyocyanin (PYO), (hence the common name of "*Bacillus pyocyaneus*"). Such a specificity from *P. aeruginosa* has recently orientated the idea of using electrochemistry to detect the presence of the bacterium in culture media [7–12]. Additionally, more recent works showed that *P. aeruginosa* is able to generate a range of redox active species that could be used as biomarkers of the bacterial presence: (i) several molecules of phenazine family as PYO: the phenazine-1-carboxylic acid (PCA) and the phenazine-1-

carboxamide (PCN) [13–15], the 1-hydroxyphenazine (OHPHZ) [13], the 5-methylphenazine-1-carboxylic acid (5-MCA) [14,15], and the 5-methyl-7-amino-1-carboxyphenazinium betaine (aeruginosin A) [16]; (ii) two alkyl-quinolones, which have a role of chemical messengers: Pseudomonas Quinolone Signal (PQS) [17–19], and its direct precursor the 2-heptyl-4(1H)-quinolone (HHQ) [17,19]; (iii) one small volatile molecule: the 2'-aminoacetophenone (2-AA) [20].

All the above-cited molecules belong to *P. aeruginosa* quorum sensing (QS). QS includes all the mechanisms for evaluation by bacteria of their population density in order to adapt their behaviors. It relies on small molecules, the autoinducers (AIs), secreted by the bacteria during growth. When AIs concentrations reach threshold levels, specific receptors are activated and allow the expression of their target genes. There are three major interconnected QS systems in *P. aeruginosa* [21,22]. Two of them, the *las* and *rhl* systems, are based on AI molecules from the N-acylhomoserine lactones family (the N-3-oxo-dodecanoyl homoserine lactone and the N-butanoyl homoserine lactone, respectively). The AIs of the *pqs* system are HHQ and PQS that can bind to and activate the transcription factor PqsR (Fig. 1), which in turn upregulates the genes required for synthesis of all the other above-cited redox molecules [23]: the phenazines through the action on the *phz* operons [24–26] and the 2-AA [27]. *In situ* detection and identification of QS species, and particularly precursor ones, is an innovative field of research that could lead to an early detection of *P. aeruginosa* and a rapid treatment of infected patients.

Besides its ability to secrete numerous redox components in the culture supernatant, *P. aeruginosa* presents a great medical interest: it is the fourth most common bacterium responsible for nosocomial infections in Europe [28] and it infects chronically more than 70% of cystic fibrosis patients who are over eighteen [29]. We already demonstrated the interest of direct electrochemical characterization of *P. aeruginosa* culture supernatant on the reference *P. aeruginosa* strain PAO1 [30]. The electrochemical response displayed a voltamperometric fingerprint associated to the complexity of the molecular cocktail secreted by a bacterial type. At the same time [18] and following this work [19], other researchers used this concept, thus demonstrating the benefits of the electrochemical characterization.

The present work reports the supernatant electrochemical signatures of bacteria grown in batch culture. It underlines also the correlation between bacterial growth and redox biomarkers production. As it is well established that different strains of *P. aeruginosa* generate different secretomes, Das and Manefield, 2012; Dietrich et al., 2006; Lépine et al., 1622 [31–33] due to different genome contents and metabolomic pathways, we determined the electrochemical fingerprints for different *P. aeruginosa* strain supernatants and their evolution overtime. To do so, we first characterized the electrochemical response of the wild-type strain PAO1 and compared it to that of PAO1Δ*pqsA*, an isogenic mutant unable to produce any alkyl-quinolones [34]. Then, three *P. aeruginosa* strains, presenting differences in the secretome composition or secretome component concentrations, were studied to evaluate the selectivity of the electrochemical response with the bacterial strains. We chose to use square wave voltammetry (SWV) in this work, an electrochemical method more and more employed to detect pyocyanin over the last years [35–39].

2. Material and methods

2.1. Chemical and reagents

All the chemicals were purchased from Sigma-Aldrich with the highest purity grade existing and used without any further purification. Stock solutions of Pseudomonas Quinolone Signal (PQS) 12.7 mM and Pyocyanin (PYO) 8 mM were prepared in acetonitrile, aliquoted and stored in freezer (−20 °C). Working solutions were prepared by dilution of stock solutions in adequate media: phosphate buffer solution (PBS) or Lysogeny Broth (LB) medium (NaCl 10 g/L, yeast extract 5 g/L, tryptone 10 g/L).

2.2. Bacterial strains and growth conditions

P. aeruginosa strain PAO1 (Holloway collection) and its isogenic mutant PAO1Δ*pqsA* [40], PA14 (R. Kolter), PAK (D. Bradley) and mucoid cystic fibrosis (CF) CHA [40] were investigated.

The same protocol was used for PAO1, PAO1Δ*pqsA*, PA14 and PAK. The *P. aeruginosa* strains were first inoculated in 30 mL LB medium and incubated overnight at 37 °C under agitation (300 rpm). Overnight cultures were centrifuged and washed with
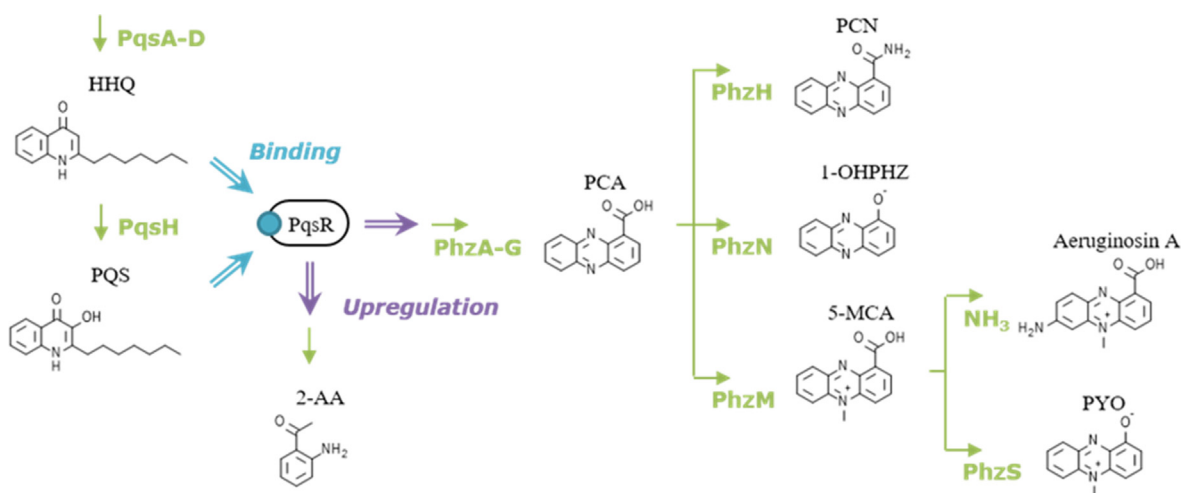
Fig. 1. Regulation scheme of the electrochemical responsive species of *P. aeruginosa*. The PqsA-D proteins produce HHQ, which is converted into PQS by the action of the PqsH enzyme. Both HHQ and PQS are the co-inducing ligands of the transcriptional regulator PqsR, which activates, among others genes, those leading to 2-AA and phenazine production. Phenazine synthesis begins by the production of PCA thanks to the action of PhzA-G proteins. Then, PCA is converted into 3 different phenazines: PCN, 1-OHPHZ and 5-MCA by action of PhzH, PhzN and PhzM enzymes, respectively. The last phenazine, 5-MCA, could be converted into aeruginosin A through the action of ammonia or into PYO through that of PhzS protein.

LB. At t_0, 1 mL of each bacterial solution was added to 155 mL of fresh LB medium to obtain an optical density at 600 nm (OD_{600}) of 0.05 (about $3·10$ [7] bacteria/mL). Then the cultures were incubated at 37 °C, 300 rpm. At 0, 2, 3, 4, 5, 6, 8, 10 and 24 h of growth, 6 mL of the medium were removed, centrifuged at 6000 rpm, passed through 0.2 μm filter and stored in ice until the electrochemical analyses were performed. In parallel, bacterial growth and supernatant pH were followed by OD_{600} spectrophotometer and a pH meter equipped with classical glass electrode, respectively.

The culture supernatant of mucoid CF CHA strain was characterized after 8 h of growth. For that, 100 mL of fresh LB medium was inoculated with washed bacteria to obtain an OD_{600} of 0.05 (about $3·10$ [7] bacteria/mL) and one sample of 10 mL was removed after 8 h of growth for analysis.

2.3. Electrochemical analysis

All electrochemical measurements were performed in a three-electrode 1.5 mL Teflon cell. The working electrode was a Glassy Carbon (GC from Methrom) electrode of 1 mm diameter, the reference electrode was a classical Ag/AgCl electrode ([KCl] 3 M) and the counter electrode was a platinum foil.

GC working electrode was polished between each measurement with a 1 μm diamond paste (RadioSpares). Then, it was rinsed with ultra-purified water and ethanol before being vortexed 2 min in ethanol and 2 min in ultra-purified water.

All electrochemical measurements were performed with a μAU-TOLAB III potentiostat (Autolab Bv, The Netherlands) equipped by Nova 1.10 software using square wave voltammetries (SWV) with the following parameters: step 5 mV, amplitude 10 mV, frequency 2 Hz (scan rate 10 mV/s). The supernatant solutions were characterized by SWV on the potential range of $-0.35/+1.2$ V, except for CHA strain analysis for which the potential range was $-0.7/+1.4$ V. The current background associated to the LB medium was measured systematically for the selected potential window before each experiment batch.

2.4. Data analysis

Data analysis was performed using Origin 9.1 software. For each culture experiment, the background current, issued from medium response, was modelled owing to a set of 8 experimental measurements situated in the flat response and in the foot of the LB response area (-0.35 to 0.60 V). Then, baselines were created for each new data from this set of 8 points. Following baseline subtraction, peak amplitude and potential were determined using multiple peaks fit function with Gauss shape in the potential range of -0.35 V/$+0.35$ V.

3. Results and discussions

3.1. LB medium electrochemical analysis

Bacteria are grown in complex media that provide nutriments required for cell growth. These media are enriched with proteins, peptones and other molecular species. These species can electrochemically react at the electrode surface leading to overestimation or/and possible hindering of *P. aeruginosa* supernatant electrochemical response. In order to enable baseline subtraction and set the electrochemical windows of the culture medium, the characterization of LB solution was performed using SWV.

The typical SWV response of LB (see Fig. S-1) is perfectly flat in the potential range from -0.35 to $+0.50$ V and presents an intense peak at a potential of $+0.85$ V. However, when repeating LB charac-

terization, the oxidation wave associated to the medium can appear at slightly less or more positive potentials. In a previous work, we showed that the main electroactive species secreted by *P. aeruginosa* are included in the potential window -0.35 to $+0.90$ V in PBS [42]. No interfering species that may induce false detection are present in LB voltammogram, in the range of PYO and PQS detection (-0.25 to $+0.52$ V). This makes possible the detection for these molecules in LB. Detection of supernatant molecules with redox potential upper than $+0.5$ V (such as the target species HHQ and 2-AA) is compromised in LB because of the presence and the non-reproducibility of the intense oxidation peak at $+0.85$ V [42]. Consequently, potentials higher than $+0.6$ V (foot of the LB wave) are not considered in this work. To characterize the *P. aeruginosa* supernatants, the boundaries of the SWV cycle are fixed in the range of -0.35 to 0.6 V.

3.2. Electrochemical spectra of PAO1 and PAO1ΔpqsA supernatants

3.2.1. Overview of the PAO1 strain spectra

The study of the electrochemical responses of *P. aeruginosa* secreted molecules was carried out by SWV in the supernatants of different bacterial cultures. Two strains were first studied: the PAO1 strain and its isogenic mutant PAO1Δ*pqsA* (which is deleted of the *pqsA* gene sequence). This sequence is mandatory to produce HHQ and PQS as presented in Fig. 1 [43]. So PAO1Δ*pqsA* strain does not produce neither HHQ and PQS nor any phenazine species that represent the main electroactive molecules secreted by *P. aeruginosa*. [14,18] Therefore, PAO1Δ*pqsA* is used in this study to corroborate peaks attribution associated to PQS production and to identify the electrochemical responses associated to secretions independent from *pqs* system.

To accurately compare the electrochemical responses of the strains, we followed their growing behavior by using optical density (OD) experiments as reference method. Inserts of Fig. 2a and b present the evolution of the culture OD at 600 nm (OD_{600}) during growth of PAO1 and PAO1Δ*pqsA* strains, respectively. Both strains follow similar temporal evolution that is usually expected for bacterial cultures, including a short lag phase, an exponential growth period and then a stationary phase.

Fig. 2a illustrates the electrochemical SWV spectra of PAO1 strain supernatant during growth. In the potential range -0.35 to $+0.60$ V, seven to nine peaks appearedgradually, the first ones as soon as 3 h of growth. The $+0.25$ to $+0.60$ V potential window is difficult to clearly analyze due to the presence of multiple peaks with significant overlapping in potential. The well-defined peaks visible in the potential range -0.35 to $+0.25$ V are numbered from 1 to 5. Fig. 3 summarizes the temporal evolution of those peak amplitudes.

Peaks 1 and 5 are assigned to PYO and PQS molecules, respectively, based on their potential value. [42] To confirm this assertion, aliquots of the two products were added to artificially increase their concentration resulting in a concomitant increase in peak intensities (data not shown). Other species of the phenazine family as PCA and PCN may be electrochemically detected at potentials close to PYO one, as reported by Bellin et al. [14]. We can rule out the presence of PCA and PCN in our sample as the shape of the peak associated to PYO near -0.25 V is symmetrical and well resolved (Fig. 2a).

Amplitude of PYO and PQS peaks increased substantially during growth, up to 10 h, then it decreased (Fig. 2a). For PQS, this result is consistent with Lépine et al. [33], who reported that PQS concentration reaches a maximum level during the early stationary phase, before decreasing. For PYO, literature shows that concentration increases from 3/5h until 9/12 h of growth [32,44]. Then, PYO concentration is reported to either remain constant, [32] or decrease [44].
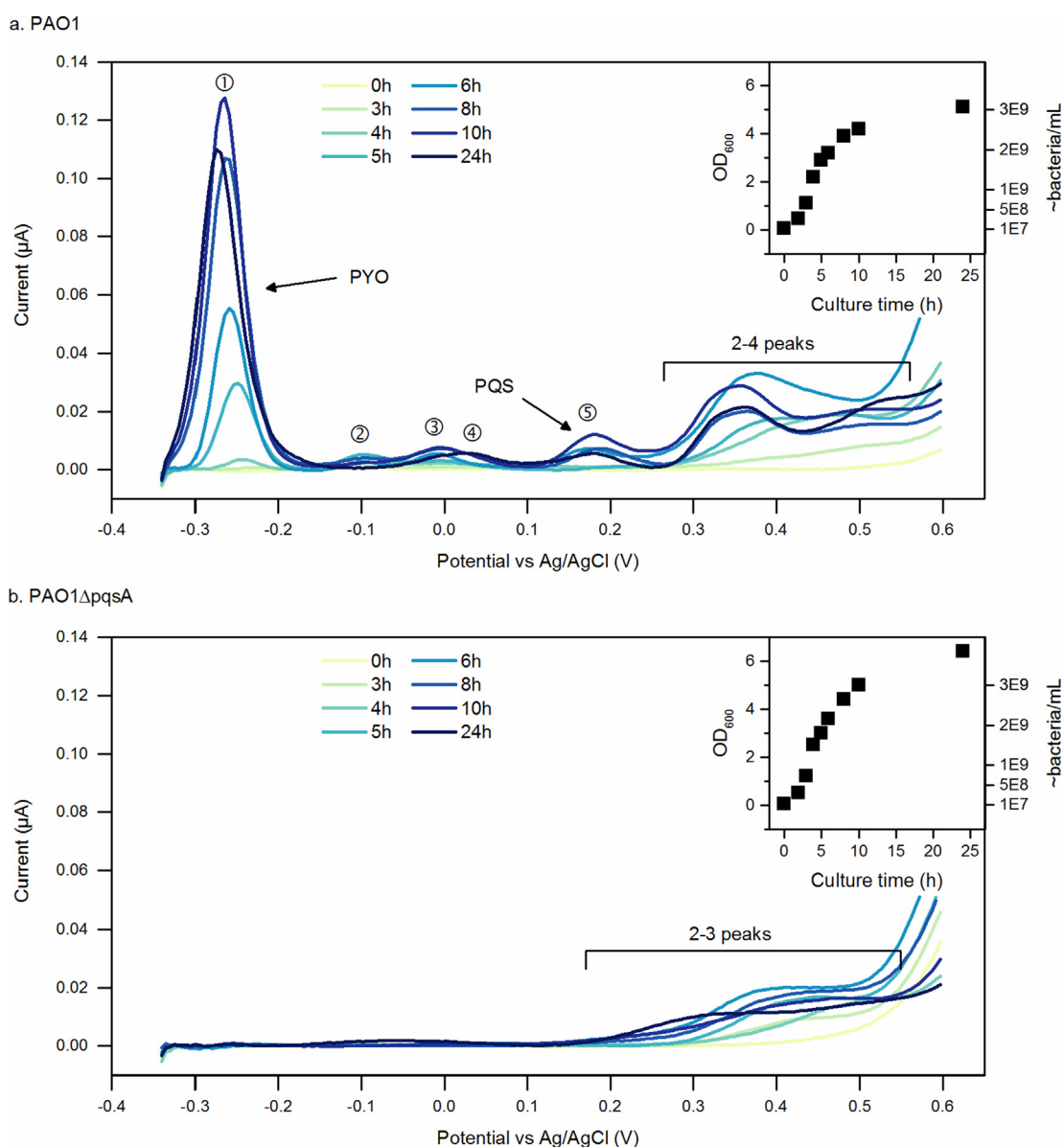
Fig. 2. Temporal evolution of the SWV responses, on glassy carbon working electrode (step 5 mV, amplitude 10 mV and frequency 2 Hz) with the supernatant of two *P. aeruginosa strains*: a. PAO1, b. PAO1Δ*pqsA*. The inserts present the temporal evolutions of OD₆₀₀ and estimated bacterial concentrations for each strain.

Peaks noted 2, 3 and 4, detected in the potential window −0.15 to +0.10 V (Fig. 2a), are not related to classically studied redox species issued from *P. aeruginosa* QS. Peaks 2 and 3 reached also a maximum before falling in current as already seen for PYO and PQS during the bacterial growth. This suggests that the aforementioned species are under control of QS. From Bellin et al. [15] results and according to its potential value, peak 3 may correspond to 5-MCA. Concerning peak 4, it appeared late, after 8 h of growth (Fig. 3): it might correspond to products of degradation coming from secreted species since its appearance was concomitant with the inflection of the peak amplitude of PYO, PQS and that of peak 3.

To verify the specificity of the SWV response to PAO1 secretions, PAO1Δ*pqsA* mutant (which is impaired in HHQ and PQS production, and, consequently, does not produce any phenazines[34]) was assayed (Fig. 2b). As expected, the voltamperometric response of the mutant supernatant markedly differs from the one of PAO1 (Fig. 2a). No response is observed in the −0.35 to +0.25 V area where PQS and phenazines are normally detectable. From this analysis, we could conclude that all the species detected in the

aforementioned range are dependent on *pqsA* expression, the unknown species corresponding to peaks 2, 3 and 4 included. Contrary to the electrochemical response in the −0.35 to +0.25 V potential range, a complex voltamperometric response is observable in the +0.25 to +0.60 V range including 2–3 different peaks. So, PAO1 strains seem to produce electrochemical species that are not dependent of the *pqsA*–encoded enzyme. It is important to notice that these peaks were not yet identified in the literature. However, their attribution is out of the scope of this work and would be the aim of further studies.

Interestingly, our experiments highlight the complex electrochemical response of secreted species in *P. aeruginosa* strain supernatants over a large potential window. In the literature, PYO is generally considered as the main electrochemical target in *P. aeruginosa* supernatant due to its response amplitude and reversibility. For example, the pioneering works of Bukelman et al. [8] showed that PYO is the unique electrochemically responsive species of PAO1 supernatant grown in LB over a potential window ranging from −0.7 to +0.6 V using cyclic voltammetry (CV). In
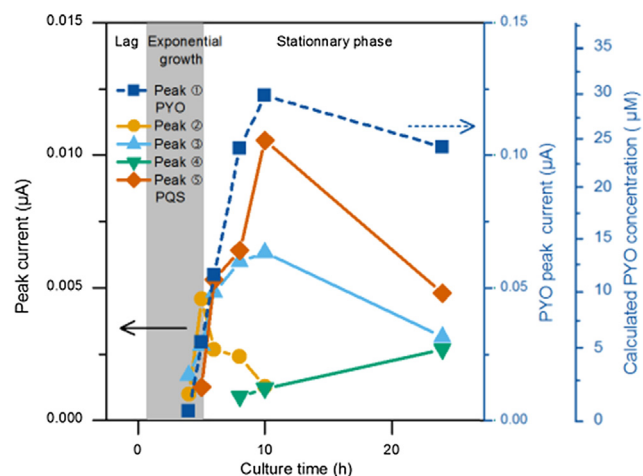
Fig. 3. Temporal evolution of the peaks amplitudes recorded in supernatant for PAO1 culture.

fact, at the exception of PYO response, the other peaks observable in Fig. 2a exhibit rather low amplitude and may be partially or totally hidden by background signal and capacitive current in CV experiments. Indeed, pulsed electrochemical methods (e.g. square wave and differential pulse voltammetries) provide strong advantage over CV to efficiently extract the electrochemical response from the capacitive and background currents. Recently, four other works were published and explored large potential range using pulsed voltametries [14,15,18,19]. Bellin and co-workers [14,15] made their detection by SWV on −0.8 to +0.2 V range at 50 Hz or 10 Hz. They did not observe any other peaks than those corresponding to PYO and phenazines (PCN, PCA and 5-MCA). Indeed, the utilized pulsing frequencies are too high for the characterization of slow redox reactions as PQS one. Morever, the electrochemical window is not sufficiently extended for exploiting other existing signals at more anodic potentials [42]. Seviour et al. [18] studied the PAO1 strain on −0.4 to +0.4 V potential range with differential pulse voltammetry (DPV). However, only PYO and PQS responses were found in the supernatant. Indeed, DPV is a well-adapted technique to subtract capacitive and background currents for the study of irreversible signals but does not amplify reversible signals as SWV. So weak signals could be missed out. Buzid et al. [19] studied PA supernatant on boron-doped diamond (BDD) electrode using DPV on −0.35 to +1.5 V range. They detected PYO, PQS and HHQ after physicochemical extraction from the supernatant medium and redissolution in a exogenous analyte (mixture 20–80% in volume respectively of acetonitrile and aqueous acetate buffer 50 mM, pH 5.0,). The obtained voltammograms also show the presence of two non-identified shoulders near −0.1 V and +0.1 V that are not discussed in the paper. All these reasons could explain why we observed more peaks in our experiments than in the ones that were already published.

3.2.2. Evolution of the PYO and PQS peaks

To evaluate the concentration of PYO and PQS present in the supernatant, calibration curves obtained within LB medium are needed.

PYO calibration curves were made in triplicate in LB for concentrations ranging from 0.5 to 100 μM by using the same SWV experimental parameters than those used for supernatant characterization (Fig. S-2). Contrary to the linear calibration curves obtained in PBS buffer [42], an allotropic behavior was observed that could be explained by a matrix effect of LB medium that contains a complex cocktail of molecular and proteinaceous compo-

nents. This allotropic behavior was already reported for calibration in Muller Hinton medium [5]. Nevertheless, this calibration enables us to determine the concentrations of PYO in the supernatant as reported in Fig. 3. The maximum of PYO concentration was obtained after 10 h of culture and corresponds to 29.7 μM. This value is of the same order of magnitude than the ones previously reported in the literature [32,45]. However, it is important to note that this value is strongly dependent on culture conditions (for example after 10 h of PAO1 culture, PYO concentration was estimated at 6 μM for an OD_{600} equal to 2.2 in LB [32] and 60 μM for an OD_{600} equal to 2 in peptone broth [45]) and on cell strain variability.

We also studied in a previous work the electrochemical behavior of PQS in PBS leading to its calibration curve in the concentration range 0–60 μM [42]. This calibration curve is accurately obtained for concentrations lower than 20 μM whereas, for higher concentrations, large variance is observed. This behavior reflects the poor solubility of PQS in aqueous solution leading to its rapid adsorption on the electrochemical cell surface as already reported by Lépine et al. [33]. Such behavior is also demonstrated by the decrease in signal amplitude observed over time in PBS for PQS (10 μM), as determined by SWV (Fig. S-3, 20% of the signal was lost after 25 min of measurement). Surprisingly, PQS exhibits more dramatic instability in LB medium free of bacteria leading to the complete disappearance of response less than 5 min after addition (Fig. S-3). Such behavior was already reported by Calfee et al. [46] for peptone Trypticase Soy Broth medium. It may correspond to interaction with constitutive proteins of the medium (that would decrease PQS availability and diffusivity). Therefore, PQS calibration in bacteria-free LB is impossible.

However, as displayed in Fig. 2a and b, contrary to the results obtained in bacteria-free LB, the PQS peak was recorded in *P. aeruginosa* supernatant. Indeed, such behavior in LB medium containing bacteria is explained by solubilization of PQS by the rhamnolipids [46], a surfactant secondary metabolites produced by *P. aeruginosa*. However, the electrochemical response of PQS appears rather weak (10 μA after 10 h culture, Fig. 3) in comparison to PYO (150 μA–30 μM- after 10 h culture, Fig. 3). In fact, some quantification issued from MS measurements shown that PQS could rise concentrations as high as 323 μM after 8 h culture for PAO Strain [47]. Such a lower amplitude could be explained by two concomitant phenomena: first a large ratio of PQS remained bound to the bacterial membranes Lépine et al. [33] and is therefore poorly detectable using electrochemistry and, secondly, free PQS exhibits reduced diffusivity and accessibility due to rhamnolipids complexation. These phenomena could explain the impossibility to detect PQS using cyclic voltammetry in Bukelman et al. [8] works.

As it is not possible to make a calibration curve in bacteria-free LB, the quantification of PQS concentration in supernatants is only possible through standard addition method. As already explained above, 2 aliquots of PQS were added to the 24 h growth supernatant (after sampling from the cell culture) to confirm the attribution of peak 5 to the PQS response. Through this method, an estimated value of 9 μM is obtained for PAO1-secreted PQS after 24 h of growth. This concentration is of the same order of magnitude than that already reported for PAO1 strain: between 7 μM (after 20 h of culture in modified ABTG medium, LC/MS determination) [18] and 55 μM (after 24 h of culture in LB medium, HPLC determination) [48].

One can notice in Fig. 2a the cathodic shift of the PYO peak potential measured in PAO1 supernatant during growth (from −0.24 to −0.27 V). The electrochemical oxidation mechanism of PYO exchanges two electrons and two protons. Thereby, according to the Nernst law, the electrochemical potential of PYO exhibits a linear pH dependency with a slope of 59 mV/decade for a reversible redox system. Consequently, the cathodic displacement of the

PYO wave can be attributed to the alkalinization of the LB medium during bacterial growth as already reported. [49] By taking pH 7 as a reference point and the theoretical slope of −59 mV/decade, we can calculate the supernatant pH from PYO peak potential displacement. The pH variation calculated from PYO peak evolution over time fits rather well the pH measured in the supernatant using a pH glass-electrode (Fig. 4). Moreover, the pH temporal evolution curves fits well the evolution of the OD_{600} of PAO1 strain culture (Fig. 4). So, pH evolution seems to be homothetic with the numbers of bacteria in the medium. As a consequence, *P. aeruginosa* bacterial growth could be estimated without need of other external measurement owing to the potential shift of PYO peak.

3.2.3. Is the electrochemical spectrum specific from a bacterial strain?

Our data on PAO1 and PAO1Δ*pqsA* supernatants clearly show the different electrochemical profiles that can be recorded depending on the ability of the strains to produce secondary metabolites (wild-type *vs* mutant). To validate our approach, we pursued it by analyzing the supernatants of different *P. aeruginosa* clinical isolates. These isolates were chosen since they are extensively studied in the literature and known to produce different amounts of secondary metabolites due to different genetic backgrounds. Hence, the clinical isolate PA14, which exhibits higher virulence in various infection models compared to the PAO1 strain [50], was also reported to produce more PYO than PAO1 [31,32]. Another valuable strain is the PAK isolate that is known to be a poor producer of PYO and unable to secrete PQS molecule Lépine et al. [33]. The last strain we used is the CF isolate CHA, a mucoid strain that secretes alginate [41]. The characteristic of this strain is to produce colonies exhibiting a reddish color on *Pseudomonas* Isolation Agar plate [51], instead of the blue-green color observed for the other strains mentioned above. The associated pigment is not clearly identified, but is presumably a phenazine derivative and thus may be detected using electrochemistry.

Fig. 5 displays the temporal OD_{600} evolutions (insert) of the culture media and the electrochemical SWV responses obtained for all the *P. aeruginosa* strain supernatants after 8 h of culture. All the studied strains exhibits similar growth based on the OD temporal evolution. The SWV voltammograms clearly exhibit marked differences in terms of peak amplitudes (PAO1 *vs* PA14) or peak repartition (PAO1 and PA14 *vs* PAK and CHA).

The electrochemical response obtained for PA14 is very similar to that of PAO1 (Figs. 5 and S-4). Similar distribution of current

peaks is obtained at the same potentials with a marked predominance of PYO and PQS peaks as already observed for PAO1. The electrochemical responses of PQS and PYO (Fig. S-5) follow the same evolution over time for both strains with a first detection at around 4 h. As already seen for PAO1, PYO and PQS responses decrease markedly after 10 h of growth. However, PA14 response is clearly higher for PQS and PYO biomarkers. Indeed, the ratio between PA14 and PAO1 peak maximum for PYO takes a value of 2.7. This higher PYO production is consistent with previous measurements, using classical biochemical detection tools [31,32]. The maximum of PQS electrochemical response is 3 times higher for PA14 than PAO1. But, the amount of PQS produced by the two strains is more controversial in the literature since higher or similar PQS levels were reported for PA14 [47] and PAO1 Lépine et al., 1622 [33] in previous works. This first experiment shows that the electrochemical detection of redox biomarkers enables us to differentiate two strains exhibiting marked difference in PYO and PQS production.

As expected, the electrochemical SWV spectrum of PAK supernatant (Fig. 5) does not reveal the presence of any PQS nor PYO, but one peak (peak 7) iss identified at a potential of +0.38 V: its amplitude increased from 3 to 6 h before falling down after 10 h (Fig. S-6a and b). This component may correspond to the one present in the unidentified potential area of PAO1, PA14 and PAO1Δ*pqsA*. Nevertheless, after a longer time of growth, a new component (peak 6) appeared at +0.24 V while the former +0.38 V peak completely disappeared. This peak is highly specific of PAK strain since no peak is observed for the other strains at this potential. Unfortunately, we are not able to clearly attribute these electrochemical responses to specific redox species. No peak is observed in PAK supernatant in the −0.35 to +0.2 V range, where PYO and PQS are usually detected.

The SWV response of the CHA supernatant (Fig. 5) shows marked differences with the electrochemical SWV spectra of PAO1 and PA14 strains, as expected. The peaks 1, 2, 3 and 5 already observed for PAO1 are clearly present but with different amplitudes (peak 4 is absent here but is generally under the limit of detection at 8 h for PAO1). Peak 1 corresponding to PYO is highly depleted whereas peaks 2 and 3 are markedly enhanced in intensity, peak 2 being the main component of the signal. PQS response (peak 5) remains at a level similar to that measured with PAO1. Moreover, one new broad peak (peak 8) appears at a lower potential than that of PYO (−0.32 V). According to the peak potential, this component may be attributed to another phenazine that have close half-wave potential including PCA (−0.31 V) [13], PCN (−0.34 V) [13] or aeruginosin A (−0.34 V) [15]. On the potential range +0.30 to +0.55 V, only one peak appears at a potential similar to that of peak 7 already observed for PAK.

All the data clearly indicate that our electrochemical method is a powerful tool to analyze the electrochemical response of *P. aeruginosa* strain supernatants in rich medium, and to identify different patterns linked to differences in secondary metabolites produced by the strains. Therefore, SWV analysis of *P. aeruginosa* strain supernatants may be implemented as fast and simple screening methodology for either identification of the exoproducts secreted by an unknown *P. aeruginosa* strain, evaluation of the *P. aeruginosa* strain diversity present in a biological sample of interest or detection of a specific *P. aeruginosa* strain owing to its exoproduct fingerprint. Nevertheless, further works are still needed to obtain a complete ID card of the *P. aeruginosa* supernatant electrochemical signature. This requires first the identification of all the redox species associated to the bacterial strains of interest by mass spectrometry and secondly the electrochemical characterization of an enlarged *P. aeruginosa* strain database.
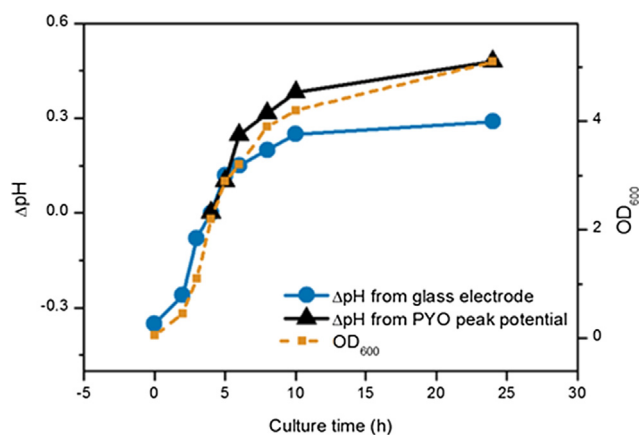

Fig. 4. Temporal evolution of the pH measured by glass electrode and of the pH calculated from the shift in potential of the PYO peak potential and of OD_{600} for the PAO1 culture in LB.
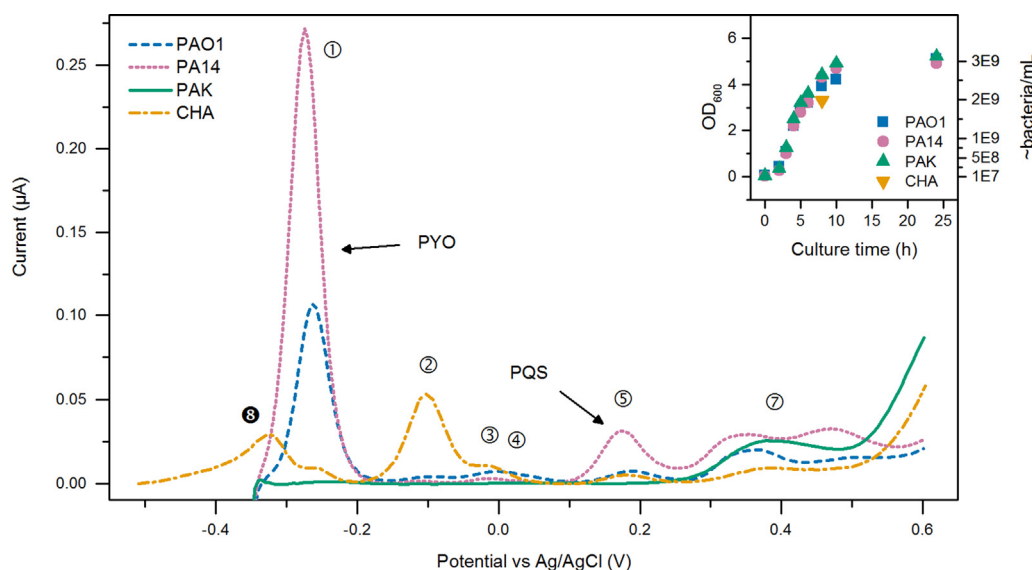
Fig. 5. Comparison of the SWV responses (step 5 mV, amplitude 10 mV and frequency 2 Hz) on Glassy Carbon working electrode of PAO1, PA14, PAK and CHA supernatants after 8 h of growth. Insert: temporal evolution of OD600 and corresponding bacterial concentrations.

4. Conclusions

Direct electrochemical analysis of supernatant (without further purification and/or extraction) of several *P. aeruginosa* strains grown in LB medium was performed with success in this work. First, supernatants of the reference strain PAO1 were analyzed by SWV techniques all along the growth. The obtained voltammograms exhibit a complex electrochemical response composed of at least 7 redox peaks that are the electrochemical image of the secretome complexity. Among them, two intense and well-defined peaks are assigned to PYO and PQS. Their temporal evolutions as well as their concentrations are in good accordance with results reported in the literature by LC-MS or HPLC methods. Thus, the electrochemical analysis allows easy and fast detection of these two *P. aeruginosa* important metabolites. Beyond that, all the peaks observed on the voltammograms and their temporal evolution constitute the electrochemical ID-card of PAO1 strain. It could be used as a signature to recognize this strain but also, by extension, to discriminate mutant strains that intrinsically generate their own secretome in terms of species concentrations and/or nature.

To verify this assertion, we analyzed the electrochemical response of supernatants issued from the culture of different *P. aeruginosa* strains. The study of the supernatants of the isogenic mutant PAO1Δ*pqsA* shows that most of the peaks detected in the PAO1 supernatant are dependent on the *pqs* operon, as expected. But peaks over +0.3 V are still present in the mutant supernatant. This suggests that bacteria, which do not possess functional *pqs* system, could also produce interesting redox species usable to detect them by electrochemistry. We compared the supernatants of 3 others *P. aeruginosa* clinical strains: PA14, PAK, CHA. Our data demonstrate that the electrochemistry is an efficient tool to identify different metabolites production patterns. In conclusion, electrochemical analysis of bacterial supernatant could provide a quick and easy way to visualize the main redox secreted species of an unknown PA strain. This information could be useful, for example, for researchers to find easily strains with original metabolome and, in the future, to clinicians in order to choose the best antibiotherapy.

In the second part of this study, we will describe an effective detection of the secretome of *Pseudomonas Aeruginosa* thanks to a non-conventional electrode material, PEDOT:PSS.

Author contributions

Conception of the work, data analysis and interpretation and drafting the article, critical revision of the article: JO, SE and PM. Data collection: JO and SE. Final approval of the version to be published: all the authors.

Declaration of Competing Interest

The authors declare that they have no known competing financial interests or personal relationships that could have appeared to influence the work reported in this paper.

Acknowledgment

Appendix A. Supplementary material

The Supporting Information is available on the ACS Publications website as a pdf file that contains the Figs. S-1–S-6 reported in text. Supplementary data to this article can be found online at https://doi.org/10.1016/j.bioelechem.2021.107747.

References

[1] J. O'Neill, Review on antimicrobial resistance, 2015.

[2] M.B. Miller, B.L. Bassler, Quorum sensing in bacteria, Annu. Rev. Microbiol. 55 (2001) 165–199, https://doi.org/10.1146/annurev.micro.55.1.165.

[3] L.C.M. Antunes, R.B.R. Ferreira, M.M.C. Buckner, B.B. Finlay, Quorum sensing in bacterial virulence, Microbiology 156 (2010) 2271–2282, https://doi.org/10.1099/mic.0.038794-0.

[4] M.J.J.B. Sibbald, A.K. Ziebandt, S. Engelmann, M. Hecker, A. de Jong, H.J.M. Harmsen, G.C. Raangs, I. Stokroos, J.P. Arends, J.Y.F. Dubois, J.M. van Dijl, Mapping the pathways to staphylococcal pathogenesis by comparative secretomics, Microbiol. Mol. Biol. Rev. 70 (2006) 755, https://doi.org/10.1128/MMBR.00008-06.

[5] D. Wehmhöner, S. Häussler, B. Tümmler, L. Jänsch, F. Bredenbruch, J. Wehland, I. Steinmetz, Inter- and intraclonal diversity of the pseudomonas aeruginosa

proteome manifests within the secretome, J. Bacteriol. 185 (2003) 5807, https://doi.org/10.1128/JB.185.19.5807-5814.2003.

[6] F. Lépine, S. Milot, E. Déziel, J. He, L.G. Rahme, Electrospray/mass spectrometric identification and analysis of 4-hydroxy-2-alkylquinolines (HAQs) produced by Pseudomonas aeruginosa, J. Am. Soc. Mass Spectromet. 15 (2004) 862–869, https://doi.org/10.1016/j.jasms.2004.02.012.

[7] D.V. Vukomanovic, D.E. Zoutman, G.S. Marks, J.F. Brien, G.W. van Loon, K. Nakatsu, Analysis of pyocyanin from Pseudomonas aeruginosa by adsorptive stripping voltammetry, J. Pharmacol. Toxicol. Methods 36 (1996) 97–102, https://doi.org/10.1016/S1056-8719(96)00104-9.

[8] O. Bukelman, N. Amara, R. Mashiach, P. Krief, M.M. Meijler, L. Alfonta, Electrochemical analysis of quorum sensing inhibition, Chem. Commun. (2009) 2836–2838, https://doi.org/10.1039/B901125K.

[9] T.A. Webster, H.J. Sismaet, J.L. Conte, I.J. Chan, E.D. Goluch, Electrochemical detection of Pseudomonas aeruginosa in human fluid samples via pyocyanin, Biosens. Bioelectron. 60 (2014) 265–270, https://doi.org/10.1016/j.bios.2014.04.028.

[10] H.J. Sismaet, A. Banerjee, S. McNish, Y. Choi, M. Torralba, S. Lucas, A. Chan, V.K. Shanmugam, E.D. Goluch, Electrochemical detection of Pseudomonas in wound exudate samples from patients with chronic wounds, Wound Repair Regener. 24 (2016) 366–372, https://doi.org/10.1111/wrr.12414.

[11] Y. Yang, Y.-Y. Yu, Y.-Z. Wang, C.-L. Zhang, J.-X. Wang, Z. Fang, H. Lv, J.-J. Zhong, Y.-C. Yong, Amplification of electrochemical signal by a whole-cell redox reactivation module for ultrasensitive detection of pyocyanin, Biosens. Bioelectron. 98 (2017) 338–344, https://doi.org/10.1016/j.bios.2017.07.008.

[12] A.A. Elkhawaga, M.M. Khalifa, O. El-badawy, M.A. Hassan, W.A. El-Said, Rapid and highly sensitive detection of pyocyanin biomarker in different Pseudomonas aeruginosa infections using gold nanoparticles modified sensor, PLoS ONE 14 (2019) e0216438, https://doi.org/10.1371/journal.pone.0216438.

[13] Y. Wang, D.K. Newman, Redox Reactions of Phenazine Antibiotics with Ferric (Hydr)oxides and Molecular Oxygen, Environ. Sci. Technol. 42 (2008) 2380–2386, https://doi.org/10.1021/es702290a.

[14] D.L. Bellin, H. Sakhtah, J.K. Rosenstein, P.M. Levine, J. Thimot, K. Emmett, L.E.P. Dietrich, K.L. Shepard, Integrated circuit-based electrochemical sensor for spatially resolved detection of redox-active metabolites in biofilms, Nat. Commun. 5 (2014) 3256, https://doi.org/10.1038/ncomms4256.

[15] D.L. Bellin, H. Sakhtah, Y. Zhang, A. Price-Whelan, L.E.P. Dietrich, K.L. Shepard, Electrochemical camera chip for simultaneous imaging of multiple metabolites in biofilms, Nat. Commun. 7 (2016) 10535, https://doi.org/10.1038/ncomms10535.

[16] E.A. Abu, S. Su, L. Sallans, R.E. Boissy, A. Greatens, W.R. Heineman, D.J. Hassett, Cyclic voltammetric, fluorescence and biological analysis of purified aeruginosin A, a secreted red pigment of Pseudomonas aeruginosa PAO1, Microbiology (Reading, England) 159 (2013) 1736–1747, https://doi.org/10.1099/mic.0.065235-0.

[17] L. Zhou, J.D. Glennon, J.H.T. Luong, F.J. Reen, F. O'Gara, C. McSweeney, G.P. McGlacken, Detection of the Pseudomonas Quinolone Signal (PQS) by cyclic voltammetry and amperometry using a boron doped diamond electrode, Chem. Commun. 47 (2011) 10347–10349, https://doi.org/10.1039/C1CC13997E.

[18] T. Seviour, L.E. Doyle, S.J.L. Lauw, J. Hinks, S.A. Rice, V.J. Nesatyy, R.D. Webster, S. Kjelleberg, E. Marsili, Voltammetric profiling of redox-active metabolites expressed by Pseudomonas aeruginosa for diagnostic purposes, Chem. Commun. 51 (2015) 3789–3792, https://doi.org/10.1039/C4CC08590F.

[19] A. Buzid, F. Shang, F.J. Reen, E.Ó. Muimhneacháin, S.L. Clarke, L. Zhou, J.H.T. Luong, F. O'Gara, G.P. McGlacken, J.D. Glennon, Molecular signature of pseudomonas aeruginosa with simultaneous nanomolar detection of quorum sensing signaling molecules at a boron-doped diamond electrode, Sci. Rep. 6 (2016) 30001, https://doi.org/10.1038/srep30001.

[20] J.P. Metters, D.K. Kampouris, C.E. Banks, Electrochemistry provides a point-of-care approach for the marker indicative of Pseudomonas aeruginosa infection of cystic fibrosis patients, Analyst 139 (2014) 3999–4004, https://doi.org/10.1039/C4AN00675E.

[21] S.P. Diggle, P. Cornelis, P. Williams, M. Cámara, 4-Quinolone signalling in Pseudomonas aeruginosa: Old molecules, new perspectives, Int. J. Med. Microbiol. 296 (2006) 83–91, https://doi.org/10.1016/j.ijmm.2006.01.038.

[22] S.L. McKnight, B.H. Iglewski, E.C. Pesci, The Pseudomonas Quinolone Signal Regulates rhl Quorum Sensing in Pseudomonas aeruginosa, J. Bacteriol. 182 (2000) 2702, https://doi.org/10.1128/JB.182.10.2702-2708.2000.

[23] H. Cao, G. Krishnan, B. Goumnerov, J. Tsongalis, R. Tompkins, L.G. Rahme, A quorum sensing-associated virulence gene of Pseudomonas aeruginosa encodes a LysR-like transcription regulator with a unique self-regulatory mechanism, Proc Natl. Acad. Sci. USA 98 (2001) 14613, https://doi.org/10.1073/pnas.251465298.

[24] E. Déziel, S. Gopalan, A.P. Tampakaki, F. Lépine, K.E. Padfield, M. Saucier, G. Xiao, L.G. Rahme, The contribution of MvfR to Pseudomonas aeruginosa pathogenesis and quorum sensing circuitry regulation: multiple quorum sensing-regulated genes are modulated without affecting lasRI, rhlRI or the production of N-acyl- l-homoserine lactones, Mol. Microbiol. 55 (2005) 998–1014, https://doi.org/10.1111/j.1365-2958.2004.04448.x.

[25] S.P. Diggle, K. Winzer, S.R. Chhabra, K.E. Worrall, M. Cámara, P. Williams, The Pseudomonas aeruginosa quinolone signal molecule overcomes the cell density-dependency of the quorum sensing hierarchy, regulates rhl-dependent genes at the onset of stationary phase and can be produced in the absence of LasR, Mol. Microbiol. 50 (2003) 29–43, https://doi.org/10.1046/j.1365-2958.2003.03672.x.

[26] P. Nadal Jimenez, G. Koch, J.A. Thompson, K.B. Xavier, R.H. Cool, W.J. Quax, The multiple signaling systems regulating virulence in Pseudomonas aeruginosa, Microbiol. Mol. Biol. Rev. 76 (2012) 46, https://doi.org/10.1128/MMBR.05007-11.

[27] M. Kesarwani, R. Hazan, J. He, Y. Que, Y. Apidianakis, B. Lesic, G. Xiao, V. Dekimpe, S. Milot, E. Deziel, F. Lépine, L.G. Rahme, A quorum sensing regulated small volatile molecule reduces acute virulence and promotes chronic infection phenotypes, PLoS Pathog. 7 (2011) e1002192, https://doi.org/10.1371/journal.ppat.1002192.

[28] European Centre for Disease Prevention and Control. Surveillance Report - Point prevalence survey of healthcare-associated infections and antimicrobial use in European long-term care facilities 2013, 2013.

[29] Cystic Fibrosis Foundation. Patient Registry - Annual Data Report to the Center Directors 2013, 2013.

[30] J. Oziat, S. Elsen, R. M. Owens, G. G. Malliaras, P. Mailley, Electrochemistry provides a simple way to monitor Pseudomonas aeruginosa metabolites, in: 2015 37th Annual International Conference of the IEEE Engineering in Medicine and Biology Society (EMBC), 2015, pp. 7522–7525. 10.1109/EMBC.2015.7320132.

[31] T. Das, M. Manefield, Pyocyanin Promotes Extracellular DNA Release in Pseudomonas aeruginosa, PLoS ONE 7 (2012) e46718, https://doi.org/10.1371/journal.pone.0046718.

[32] L.E.P. Dietrich, A. Price-Whelan, A. Petersen, M. Whiteley, D.K. Newman, The phenazine pyocyanin is a terminal signalling factor in the quorum sensing network of Pseudomonas aeruginosa, Mol. Microbiol. 61 (2006) 1308–1321, https://doi.org/10.1111/j.1365-2958.2006.05306.x.

[33] F. Lépine, E. Déziel, S. Milot, L.G. Rahme, A stable isotope dilution assay for the quantification of the Pseudomonas quinolone signal in Pseudomonas aeruginosa cultures, Biochimica et Biophysica Acta (BBA) – Gen. Subj. 1622 (2003) 36–41, https://doi.org/10.1016/S0304-4165(03)00103-X.

[34] C. Pustelny, A. Albers, K. Büldt-Karentzopoulos, K. Parschat, S.R. Chhabra, M. Cámara, P. Williams, S. Fetzner, Dioxygenase-mediated quenching of quinolone-dependent quorum sensing in Pseudomonas aeruginosa, Chem. Biol. 16 (2009) 1259–1267, https://doi.org/10.1016/j.chembiol.2009.11.013.

[35] F.A. Alatraktchi, J.S. Noori, G.P. Tanev, J. Mortensen, M. Dimaki, H.K. Johansen, J. Madsen, S. Molin, W.E. Svendsen, Paper-based sensors for rapid detection of virulence factor produced by Pseudomonas aeruginosa, PLoS ONE 13 (2018) e0194157, https://doi.org/10.1371/journal.pone.0194157.

[36] J. Elliott, O. Simoska, S. Karasik, J.B. Shear, K.J. Stevenson, Transparent carbon ultramicroelectrode arrays for the electrochemical detection of a bacterial warfare toxin, pyocyanin, Anal. Chem. 89 (2017) 6285–6289, https://doi.org/10.1021/acs.analchem.7b00876.

[37] R. Jarošová, S.E. Mcclure, M. Gajda, M. Jović, H.H. Girault, A. Lesch, M. Maiden, C. Waters, G.M. Swain, Inkjet-printed carbon nanotube electrodes for measuring pyocyanin and uric acid in a wound fluid simulant and culture media, Anal. Chem. 91 (2019) 8835–8844, https://doi.org/10.1021/acs.analchem.8b05591.

[38] O. Simoska, M. Sans, M.D. Fitzpatrick, C.M. Crittenden, L.S. Eberlin, J.B. Shear, K. J. Stevenson, Real-time electrochemical detection of pseudomonas aeruginosa phenazine metabolites using transparent carbon ultramicroelectrode arrays, ACS Sens. 4 (2019) 170–179, https://doi.org/10.1021/acssensors.8b01152.

[39] H.J. Sismaet, A.J. Pinto, E.D. Goluch, Electrochemical sensors for identifying pyocyanin production in clinical Pseudomonas aeruginosa isolates, Biosens. Bioelectron. 97 (2017) 65–69, https://doi.org/10.1016/j.bios.2017.05.042.

[40] S. Aendekerk, S.P. Diggle, Z. Song, N. Høiby, P. Cornelis, P. Williams, M. Cámara, The MexGHI-OpmD multidrug efflux pump controls growth, antibiotic susceptibility and virulence in Pseudomonas aeruginosa via 4-quinolone-dependent cell-to-cell communication, Microbiology 151 (2005) 1113–1125.

[41] I. Toussaint, P.M. Delicattree, Vignais, Pseudomonas aeruginosa Contains an IHF-like Protein That Binds to the algD Promoter, Biochem. Biophys. Res. Commun. 196 (1993) 416–421, https://doi.org/10.1006/bbrc.1993.2265.

[42] J. Oziat, M. Gougis, G.G. Malliaras, P. Mailley, Electrochemical characterizations of four main redox–metabolites of Pseudomonas aeruginosa, Electroanalysis 29 (2017) 1332–1340, https://doi.org/10.1002/elan.201600799.

[43] J.P. Coleman, L.L. Hudson, S.L. McKnight, J.M. Farrow, M.W. Calfee, C.A. Lindsey, E.C. Pesci, Pseudomonas aeruginosa PqsA Is an Anthranilate-Coenzyme A Ligase, J. Bacteriol. 190 (2008) 1247, https://doi.org/10.1128/JB.01140-07.

[44] V. Dekimpe, E. Déziel, Revisiting the quorum-sensing hierarchy in Pseudomonas aeruginosa: the transcriptional regulator RhlR regulates LasR-specific factors, Microbiology 155 (2009) 712–723.

[45] B.R. Lundgren, W. Thornton, M.H. Dornan, L.R. Villegas-Peñaranda, C.N. Boddy, C.T. Nomura, Gene PA2449 is essential for glycine metabolism and pyocyanin biosynthesis in Pseudomonas aeruginosa PAO1, J. Bacteriol. 195 (2013) 2087, https://doi.org/10.1128/JB.02205-12.

[46] M.W. Calfee, J.G. Shelton, J.A. McCubrey, E.C. Pesci, Solubility and bioactivity of the pseudomonas quinolone signal are increased by a Pseudomonas aeruginosa-produced surfactant, Infect. Immun. 73 (2005) 878, https://doi.org/10.1128/IAI.73.2.878-882.2005.

[47] L. Zhou, F.J. Reen, F. O'Gara, C.M. McSweeney, S.L. Clarke, J.D. Glennon, J.H.T. Luong, G.P. McGlacken, Analysis of pseudomonas quinolone signal and other bacterial signalling molecules using capillaries coated with highly charged polyelectrolyte monolayers and boron doped diamond electrode, J. Chromatogr. A 1251 (2012) 169–175, https://doi.org/10.1016/j.chroma.2012.06.064.

[48] A. Bala, R.K. Gupta, S. Chhibber, K. Harjai, Detection and quantification of quinolone signalling molecule: A third quorum sensing molecule of Pseudomonas aeruginosa by high performance-thin layer chromatography, J. Chromatogr. B 930 (2013) 30–35, https://doi.org/10.1016/j.jchromb.2013.04.027.

[49] N. Boes, K. Schreiber, M. Schobert, SpoT-triggered stringent response controls usp gene expression in Pseudomonas aeruginosa, J. Bacteriol. 190 (2008) 7189, https://doi.org/10.1128/JB.00600-08.

[50] D.G. Lee, J.M. Urbach, G. Wu, N.T. Liberati, R.L. Feinbaum, S. Miyata, L.T. Diggins, J. He, M. Saucier, E. Déziel, L. Friedman, L. Li, G. Grills, K. Montgomery, R. Kucherlapati, L.G. Rahme, F.M. Ausubel, Genomic analysis reveals that Pseudomonas aeruginosa virulence is combinatorial, Genome Biol. 7 (2006) R90, https://doi.org/10.1186/gb-2006-7-10-r90.

[51] K.M. Sall, M.G. Casabona, C. Bordi, P. Huber, S. de Bentzmann, I. Attrée, S. Elsen, A gacS Deletion in Pseudomonas aeruginosa Cystic Fibrosis Isolate CHA Shapes Its Virulence, PLoS ONE 9 (2014) e95936, https://doi.org/10.1371/journal.pone.0095936.